

CERIA BASED NANO-COMPOSITE ELECTRODES FOR INTERMEDIATE TEMPERATURE SOLID OXIDE FUEL CELLS (IT-SOFCs)

M. A. KHAN^{a*}, R. RAZA^a, M. A. CHAUDHRY^b, G. ABBAS^a, A. RAFIQUE^a,
M. K. ULLAH^a, A. ALI^a, M. N. MUSHTAQ^a

¹*Department of Physics, COMSATS Institute of Information Technology, 54000, Lahore, Pakistan;*

²*Department of Physics, Bahauddin Zakariya University (BZU), 60800, Multan, Pakistan*

The world is presently focusing the innovation and development of energy technology at the nano levels for solid oxide fuel cell (SOFC) in terms of its application, devices and materials. The composite electrodes which would be showed the excellent performance have high demands for precise issues in SOFC for research point of view. Ceria based composite electrodes LiNiCuZn-YDC (1-5) were prepared by using the NANOCOFC (nanocomposite for advanced fuel cell technology) approach. XRD analyses were showed that these electrodes have cubic structure. Its thermal and morphology studied were done by TGA and SEM techniques. Both analysis (XRD and SEM) were predicted that average crystallites size having the range of 30-80 nm. EIS technique was used to explore the polarization processes under H₂ atmosphere within the temperature range of (300-680 °C). The polarization resistance decreases from 0.19 to 0.05 Ωcm². The activation energy was measured under air and hydrogen atmospheres. The maximum power density (769.54 mWcm⁻¹) and open circuit voltage (1.02 V) were achieved at 680 °C by using the LiNiCuZn-YDC(3) oxide as anode, NSDC as electrolyte and BSCF as cathode.

(Received January 26, 2016; Accepted April 30, 2016)

Keywords: Nano Composite ceria Based Oxide Materials; Solid Oxide Fuel Cells; Polarization Resistance; Ohmic Resistance; Electrolyte; Activation Energy; Maximum Electro-Chemical Performance.

1. Introduction

Solid oxide fuel cells (SOFCs) are recognized systems for the electrochemical conversion to electricity of the chemical energy stored in gas and liquid fuels such as hydrogen, carbon monoxide, methane, coal syngas, and liquid hydrocarbon fuels (diesel, gasoline) [1, 2]. One issue that limits the commercialization of SOFC systems is related to the life of the fuel cell, which can be correlated to the high operation temperature. Nickel is an excellent catalyst for hydrogen electro-oxidation; Ni-based (Ni/YSZ or Ni/GDC) cermet anodes could produce excellent performance with hydrogen fuel at SOFC operating conditions [3, 4]. Fuel cell research is demanding new developments to adjust this technology to lower operating temperatures. The mixed (ionic and electronic) nano composite cermet electrode materials produced the excellent achievement in the fuel cell performance at intermediate temperature solid oxide fuel cells (IT-SOFCs). The application point of view, ceria is a promising candidate to reduce the operating temperature of solid oxide fuel cells (SOFCs) [5-11].

As reported in literature that NiO and CuO are well-known semiconductors with p type conductivity while the ZnO is an n-type conductor [12-15]. The electrical conductivities of these oxides are rather low. However, the lithiation reaction could notably improve their conductivities [14]. Li_{0.15}Ni_{0.45}Zn_{0.4}O_x displayed the highest conductivity of 0.1 S cm⁻¹ at 600 °C [16]. These transition metal oxides have been proven to show high catalytic activity for both hydrogen oxidation reaction and oxygen reduction reaction (redox reactions) [17-20]. Recently, Zhao [21] et

*Corresponding author: ajmalkhan@ciitlahore.edu.pk

al. reported a LTSOFC which achieved a power output of 730mWcm^{-2} at 550°C , in which the lithium transition metal oxide (LiNiCuZn oxide) was used as nano-catalytic electrode materials. LiNiCuZn oxide mixed with electrolytic material play a significant role to enhance the fuel cell performance.

The concept of mixed (ionic/electronic) composite electrodes [15], which were composed of ceria based coated materials (YDC, GDC, and SDC) with different transition metal oxides. These composite electrodes were enhanced the conductivity, decrease polarization resistance, improve the surface morphology and electro-chemical performance [14-16].

The electrode challenge in solid oxide fuel cell is that it exhibited the structural and chemical stability in both environs. Anode side having the reducing environmental behavior and while the cathode surface shows the oxidizing phenomena. The electrode was maintaining the dual conductivity and electro catalytic activity performance. Furthermore, it desires to express high electronic conductance to reduce the ohmic losses and considerable oxygen ionic conductance to encourage electrochemical reactions. There are different types of oxides with fluorite, perovskite, and pyrochlore structures have been studied as possible redox stable electrode materials [22-24].

In the present study, ceria-based mixed (ionic/electronic) nano-composite electrodes LiNiCuZn-YDC (1-5) were fabricated for the intermediate temperature solid oxide fuel cell. These electrodes exhibited chemically and structurally stable. These prepared electrodes were characterized by TGA, XRD, SEM, EIS, polarization and fuel cell performance.

2. Experimental

2.1 Synthesis of Nanocomposite LiNiCuZn-YDC Oxides Materials

With the help of NANOCOFC (nanocomposite for advanced fuel cell technology) process, high performance nanocomposite oxides electrode materials were prepared [25]. For preparation of the LiNiCuZn-YDC (1-5) electrodes, YDC and LiNiCuZn oxides were to be mixed. Li_2CO_3 , $\text{NiCO}_3 \cdot 2\text{Ni}(\text{OH})_2 \cdot 6\text{H}_2\text{O}$, $\text{CuCO}_3 \cdot 2\text{Cu}(\text{OH})_2 \cdot 6\text{H}_2\text{O}$, $\text{Zn}(\text{NO}_3)_2 \cdot 6\text{H}_2\text{O}$, $\text{Ce}(\text{NO}_3)_4 \cdot 6\text{H}_2\text{O}$, $\text{Y}_3(\text{NO}_3)_9 \cdot 9\text{H}_2\text{O}$, citric acid, ethylene glycol and deionized water were employed as preparatory raw chemicals.

In the light of solid state technique the semiconducting LiNiCu-oxide materials were prepared. For this purpose Li_2CO_3 , $\text{NiCO}_3 \cdot 2\text{Ni}(\text{OH})_2 \cdot 6\text{H}_2\text{O}$ and $\text{CuCO}_3 \cdot 2\text{Cu}(\text{OH})_2 \cdot 6\text{H}_2\text{O}$ were grounded and mixed. Then, 10 gram mixture of semiconducting LiNiCu-oxide was added into the 100 ml solution of zinc nitrate. The solution of LiNiCuZn-oxide was obtained after the stirring at 130°C for 2 hours. This solution has dual semiconducting properties (n and p types).

The YDC oxide solution was prepared by wet chemical one step co-precipitating method, which having the ion conducting behavior. This ion conducting (YDC) solution was added drop by drop in the LiNiCuZn-oxide solution. This mixture of solution was stirred at 150°C for 1 hour. Then 15 gram citric acid and ethylene glycol were added together in this mixture. Then, the above solution was stirred at 160°C for 2 hours. Until the dense gels of LiNiCuZn-YDC (1-5) composite electrodes were obtained. These gels were kept in a digital furnace and permitted to rise progressively up to 1100°C for 8 hours. Then we get the black ashes of LiNiCuZn-YDC (1-5) oxide materials. These black ashes were then ground for 20 minutes to obtain the final composite electrodes of LiNiCuZn-YDC (1-5) oxide materials. The appropriate molar ratios of LiNiCuZn-YDC (1-5) were expressed in the Table 1.1 and its flow chart is given away in Figure 1.

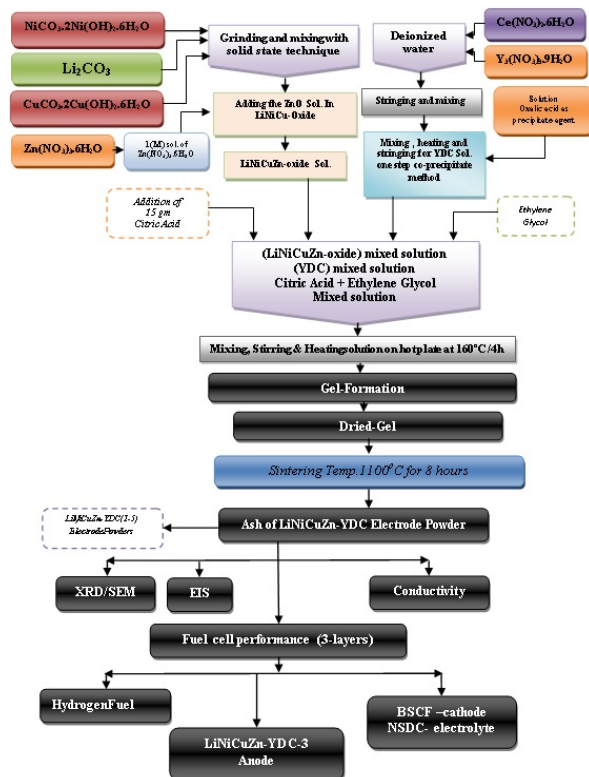


Fig.1. Flow Chart for Synthesizing LiNiCuZn-YDC Nano Composite Electrode

Table 1.1. Compositional Details of LiNiCuZn-YDC Nano-Composite Electrode Oxide Materials.

Sample Category	Compositional Name	Molar Configurations
Sample-1	LNCZ-YDC-1	$\text{Li}_{0.10}\text{Ni}_{0.20}\text{Zn}_{0.35}\text{Cu}_{0.05}-\text{Y}_{0.02}\text{Ce}_{0.28}$
Sample-2	LNCZ-YDC-2	$\text{Li}_{0.10}\text{Ni}_{0.20}\text{Zn}_{0.36}\text{Cu}_{0.04}-\text{Y}_{0.02}\text{Ce}_{0.28}$
Sample-3	LNCZ-YDC-3	$\text{Li}_{0.10}\text{Ni}_{0.20}\text{Zn}_{0.37}\text{Cu}_{0.03}-\text{Y}_{0.02}\text{Ce}_{0.28}$
Sample-4	LNCZ-YDC-4	$\text{Li}_{0.10}\text{Ni}_{0.20}\text{Zn}_{0.38}\text{Cu}_{0.02}-\text{Y}_{0.02}\text{Ce}_{0.28}$
Sample-5	LNCZ-YDC-5	$\text{Li}_{0.10}\text{Ni}_{0.20}\text{Zn}_{0.39}\text{Cu}_{0.01}-\text{Y}_{0.02}\text{Ce}_{0.28}$

2.2 Fuel Cell Fabrication

The three layer fuel cell pellets were prepared by dry pressing technique. The electrolyte NSDC was pressed between layers of the composite electrode LiNiCuZn-YDC (1-5) oxides as anode and BSCF as cathode using a hydraulic press with a load of 310 kg cm^{-2} . For a single cell test, a small pellet with a diameter of 13 mm was created, which had an active area of 0.64 cm^2 and cell thickness was measured at 1 mm. The pressed pellets were sintered at $650 \text{ }^\circ\text{C}$ for 40 min. The surfaces (anode and the cathode) of the pellets were painted with an Ag paste to improve the electrical contacts, to measure the I-V and I-P characteristics of the fuel cell.

2.3 Conductivity Measurement

For the DC conductivity measurement of the nano composite oxide material, the pellet of 13 mm in diameter with a thickness of 2.7 mm was fabricated by the dry pressing technique and sintered at $580 \text{ }^\circ\text{C}$ for 30 min. The DC conductivity was measured by KD-2531 Digital Micro-ohm Meter, China in a temperature range of $300\text{--}600 \text{ }^\circ\text{C}$ at air and hydrogen atmospheres. The silver

paste was employed on both surfaces to achieve better electrical contacts. The measured conductivities were plotted for Arrhenius plot as function of $\ln(\sigma T)$ versus $1/T$. The EIS (electrochemical impedance spectroscopy) in hydrogen atmosphere by implementing Auto VERSA STAT 2273 (Princeton Applied Research, Oak Ridge, TN). The frequency was varied from 0.1 Hz to 1 MHz.

2.4 Fuel Cell Performance

The electronic load (PLZ664WA, Kikusui) was used to measure the electrochemical performance of the cell by providing fuels at the anode side and air as oxidant at the cathode surface. The data of open circuit voltage (OCV) and current were recorded at temperature 680°C. From these results, the power density also was calculated and current versus power densities (I-P curves) were also drawn. The H₂ gas flow rate was controlled 110 ml/min at 1 atm pressure.

2.5 Characterizations

Thermo gravimetric analysis (TGA) was conducted on a Mettler Toledo TGA/SDTA 851° (Greifense, Switzerland), and the sample was heated from 25°C to 1000°C at a rate of 10°C min⁻¹ in a 70 µL alumina pan. A constant flow of nitrogen (50 ml min⁻¹) was used to provide an inert atmosphere during the pyrolysis.

Powder X-ray diffraction (XRD) patterns were recorded (PANalytical X'Pert Pro MPD, Netherlands) using CuK α radiation ($\lambda=1.5418$ Å). SEM analysis was performed (Hitachi High-Tech, S-3400 energy used between 5eV-15 kV) to observe the morphology.

3. Results and Discussion

Fig.2(a) reveals the X-rays diffraction patterns of composite LiNiCuZn-YDC (1-5) oxide materials, which were sintered at 1100°C for 8 hours. They had well crystalline structures. They are composed of CuNiZn and YDC oxides. CuNiZn-oxide with cubic structure (space group Fm-3m(225)) is observed with lattice constants of $a=3.251, b=3.251, c=3.251$, corresponding to that of JCPDS-46-1217. The diffraction peaks at 36.9, 42.9, 62.3, 74.7 and 78.6 positions can be well-assigned to (111), (200), (220), (311) and (222) planes. While, the lithium (Li) is not noticeable, this could be caused by the incorporation of Li elements to the transition metal CuNiZn-oxide. YDC-oxide with cubic structure (space group Fm-3m (225)) is observed with lattice constants of $a=4.327, b=4.327, c=4.327$, corresponding to that of JCPDS-09-0286. The diffraction peaks at 28.7, 33.2, 47.8, 56.8, 59.5, 70.0, 77.3 and 79.7 positions can be well-assigned to (111), (200), (220), (311), (222), (400), (331) and (420) planes. The indexed patterns showed that material have two phase structure and average crystallite size having the range 30-80 nm

Figure 2(b) displays the XRD patterns of LiNiCuZn-YDC-3 composite oxide material, which was sintered at 600°C, 700°C, 800°C, 900°C, 1000°C and 1100°C for 8 hours. The indexed patterns showed that the material have two phase structure. The average crystallite size of LiNiCuZn-YDC-3 oxide material which were sintered at different temperatures (600 °C-1100 °C) having the range 25-50 nm.

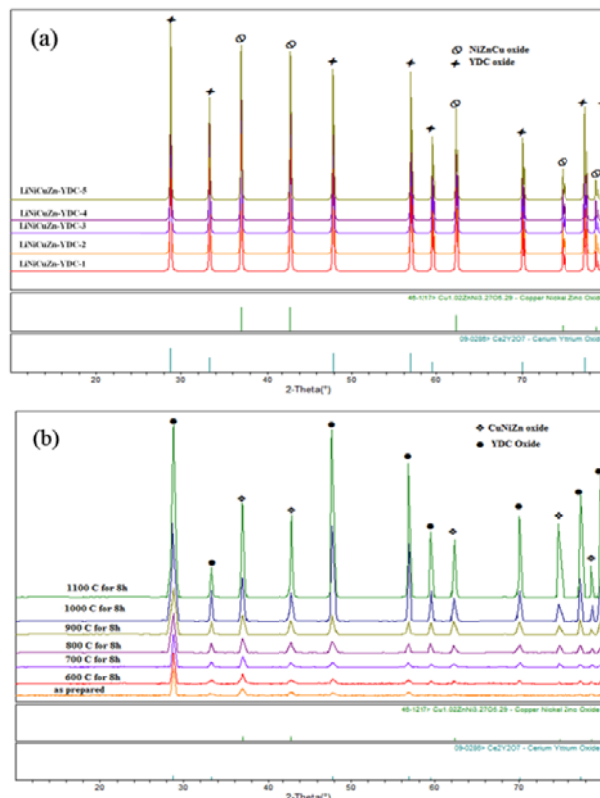


Fig.2. XRD patterns of the nano composite electrode powders. a) Nano composite electrode LiNiCuZn-YDC (1-5) sintered at 1100 °C for 8 hours; b) Nano composite electrode LiNiCuZn-YDC-3 sintered at different temperatures for 8 hours

Figure 3(a) and 3(b) show the microstructure analysis of the optimized composite LiNiCuZn-YDC-3 oxide material sintered at 1100°C for 8 hours. It has been found from the SEM image that the oxide material washomogenous, porous structure and particle size to be in range of 10-80 nm. These SEM results are comparable to those results gained from the XRD data, which further confirms that the present material possesses the nanostructure. These porous were helpful for the transportations of ions from the cathode side to anode side during the cell reaction. The cross-view image of the whole fuel cell shows in the Figure 3(c) in which LiNiCuZn-YDC-3 oxide material used as anode.

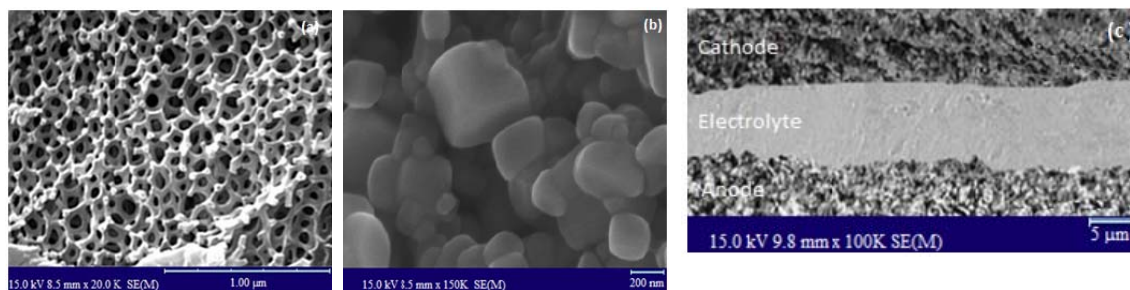


Fig.3. Microstructures analyses. a) Nano composite LiNiCuZn-YDC-3 oxide powder sintered at 1100 °C for 8 hours; b) Nano composite LiNiCuZn-YDC-3 oxide powder sintered at 1100 °C for 8 hours at high magnification; c) Cross-section analysis of fuel cell

The DC conductivity of composite LiNiCuZn-YDC (1-5) oxide materials were recorded in both environments (hydrogen and air) as a function of temperature in range of 300-600 °C. The data has been used to construct Arrhenius plots for the purpose of calculating activation energy. The results are depicted in Figures 4(a) and 4(b). It has been observed that composite LiNiCuZn-YDC-3 oxide material shows maximum results of conductivity in hydrogen and air atmospheres. It has been purposed by Zhu [30], if the conductivity of oxide material is 10 times greater than the electrolytic conductivity, then this material can be used as electrode (anode or cathode). Here, the DC conductivity of composite LiNiCuZn-YDC-3 oxide material is 10 times higher than that of NSDC electrolytic conductivity (0.1 Scm^{-1}) [31, 32]. This suggests that the composite LiNiCuZn-YDC-3 oxide material under study can be utilized for both the anode and cathode. Activation energies were estimated by linear curve fitting technique and the values obtained are shown inset the graph. It has been examined that composite LiNiCuZn-YDC-3 oxide material has lowest value of activation energies. The high catalytic activity process of the LiNiCuZn-YDC-3 is a result of low activation energy. The low value of activation energy was initially produced fast chemical reaction [33].

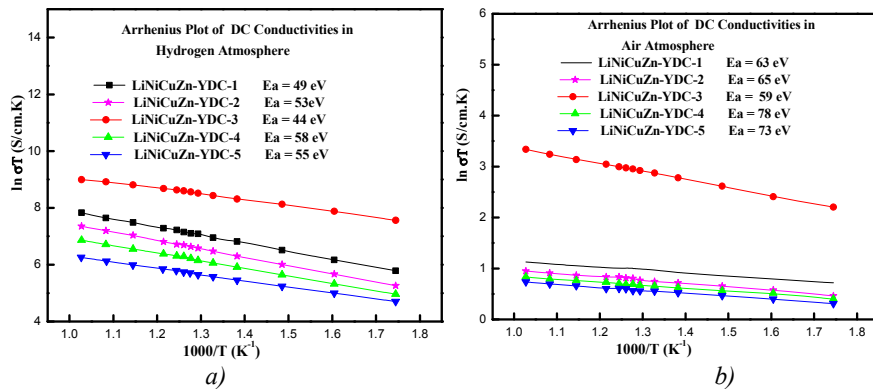


Fig.4. Arrhenius plots and Activation energy of oxide materials;
 a) DC Conductivities of LiNiCuZn-YDC-3oxide materials under H_2 atmosphere;
 b) DC Conductivities of LiNiCuZn-YDC-3oxide materials under Air surrounding

The TGA analysis of composite LiNiCuZn-YDC-3 oxide material was performed to understand the mechanism of decompositions and the formation of the final desired phase. The results are presented in Figure 5. The TG profile comprises three regions; the region-I is spanned over 25-200 °C temperature range, region- II covers 200-320 °C temperature, and region-III lies over 320-500 °C temperature. It can be seen that in region-I there is a slow weight loss due to desorption of physically absorbed water and nitrates which evaporate in this temperature region [34]. It is seen from the curve, that the region-II in the temperature range (200-320 °C) are associated with the decomposition/oxidation of process oxide phases [35]. In the region-III temperature range (320-500 °C) the combustion process occurred and required composite phase should be started [36]. But, the decomposition process ends near 1000 °C beyond at which the final oxide powder should be formed.

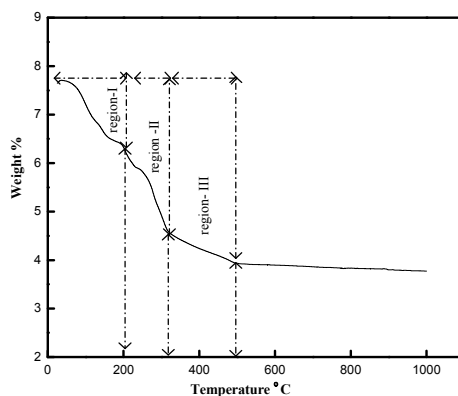


Fig.5. TGA analysis of nano composite electrode of LiNiCuZn-YDC-3

The electrochemical impedance spectroscopy (EIS) of the composite LiNiCuZn-YDC-3 oxide material was revealed in the hydrogen environment at 300-680°C. Their graphs were shown in the Figure 6. The electrode polarization and ohmic resistances were both composed in the AC impedance [37]. The intercept of high-frequency on the real axis is estimated as the ohmic resistance (R_o), including the electronic resistance of electrode, ionic resistance of the electrolyte, and some interfaces contact resistances [37]. The low frequency intercept corresponds to the total resistance (R_t), while the difference between the two (high and low intercept points) values is called the electrode polarization resistance (R_p) [38]. The magnitudes of high frequency semi-circles arch were reduced with increased of the temperature from 300 °C to 680 °C, which were related to charge transportation, mass transportation and electro catalytic activity of the surface of oxide material [37-38]. The graphical behavior showed that ohmic resistance (R_o), electrode polarization resistance (R_p) and total resistance (R_t) were reduced with the increased of temperatures. The ohmic resistance (R_o) decreases from 0.58 to 0.15 Ωcm^2 while the temperature rises from 300°C to 680°C. The total resistance (R_t) also decreases from 0.78 to 0.21 Ωcm^2 , but the electrode polarization resistance (R_p) falls from 0.19 to 0.05 Ωcm^2 . Figure 7 exposed the behavior of the polarization resistance, ohmic resistance and total resistance of composite LiNiCuZn-YDC-3 oxide material. The decrease in polarization resistance of composite LiNiCuZn-YDC-3 oxide material relates with the electro catalytic activity of the surface, charge transportation and mass transportation.

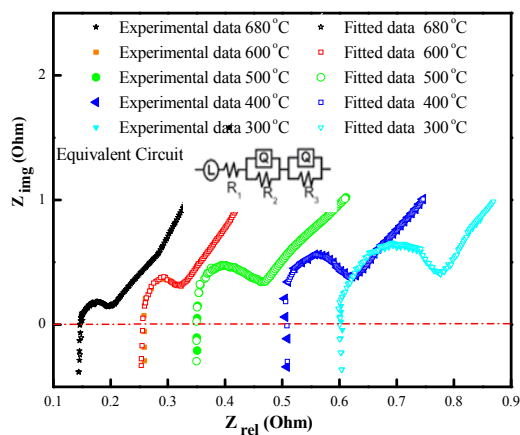


Fig.6. Electro impedance spectroscopy (EIS) analysis of nano composite of LiNiCuZn-YDC-3 oxide material under H_2 atmosphere

The electro catalytic process of the surface was improved with increased of the operating temperature form 300 °C to 680 °C. From the visual inspection of impedance data, there are “semicircle” shapes followed by “tail” evidence in H₂ atmosphere. At high frequency, there is a semi-circle zone representing fast kinetic process and catalytically active response of the reaction, and at low frequencies zone representing diffusion process occurring at the anode in hydrogen atmosphere [39-40]. This means that LiNiCuZn based oxide–Yttrium doped ceria materials have highly catalytically active and fast kinetic processes for H₂ electrochemical dissociation reactions. Further analysis of above EIS data were accomplished with the help of Z-view software, and on the base of their results, draw its equivalent circuit and shown inside the Figure 6. All the spectra contain a tail which is related to inductance effect (L). This inductance effect is allocated to the instrument leads, clamps, and stainless steel tube from the testing device [38]. Different conductance mechanisms were occurred at the electrode surface in which including the electron, oxygen ion, and proton conductions. In H₂ environment, R₁ epitomizes the ohmic resistance for proton, oxygen ion and electron due to introducing protons from H₂; R₂Q and R₃Q symbolize the charge transfer and mass transfer, respectively [41]. The fuel cell performance was also enhanced by reducing the polarization resistance in the temperature range of (300-680) °C.

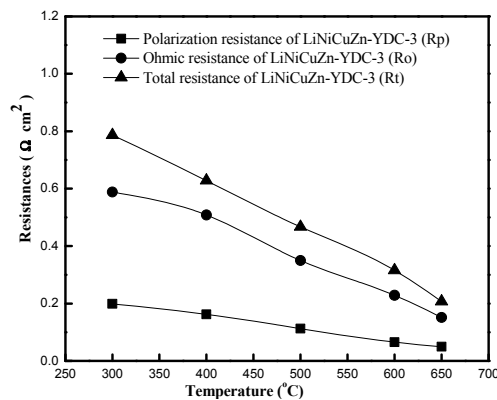


Fig.7. Polarization, Ohmic and Total resistance nano composite LiNiCuZn-YDC-3 oxide material

Five different tablets cells were prepared by utilizing with the composite oxide LiNiCuZn-YDC (1-5) materials as anodes, NSDC as electrolyte and BSCF as cathode. Their performances were measured in terms of open circuit voltage (OCV) and current at 680 °C with the help of hydrogen as a fuel at anode surface and air as oxidant at cathode surface. Their results are shown in the Figure 8(a). It can be observed from Figure 8(a) that the composite LiNiCuZn-YDC-3 oxide material based cell yields maximum power density (769.54 mWcm⁻¹) and open circuit voltage (1.02 V).

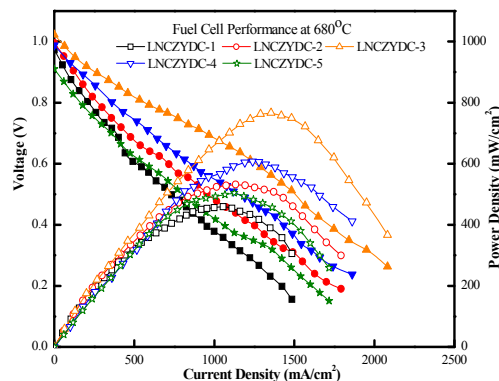


Fig.8. Electro chemical performance of cells based on LiNiCuZn-YDC (1-5) nano composite oxides as anode, NSDC as electrolyte and BSCF as cathode at 680 °C

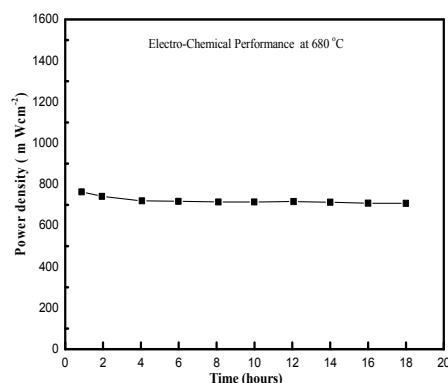


Fig.9. Short term stability of the cell with LiNiCuZn-YDC-3 nano-composite as anode, NSDC as electrolyte and BSCF as cathode

To find out the stability, the electro-chemical performance of cell (based on LiNiCuZn-YDC-3 composite oxide material as anode, NSDC as electrolyte and BSCF as cathode) was measured for 20 hours with a regular interval of an hour in five days (4 h/day). The results of measurements are revealed in the Figure 9. The degradation behavior was perceived in electro chemical performance in first 2 hours, may be owing to the electro catalytic process of the surface and transformation in morphology at anode/electrolyte interface [42-43]. The long term stability is not performed due to lack of facilities. But still for short term results are encouraging. In future, long term stability will be accomplished.

4. Conclusions

The different compositions of composite electrode LiNiCuZn-YDC (1-5) were prepared by a new approach of NANOCOFC (nanocomposite for advanced fuel cell technology). This approach is allowed the preparation of ceria based electrode in one step at relatively low cost as and at a reduced calcination temperature compared to conventional methods. This process is cost-effective, simple and practically easy to transfer to an industrial scale. Their thermogravimetric analysis (TGA), structural characteristics (XRD), scanning electron microscopic (SEM) analysis, electrochemical impedance spectroscopy (EIS), conductivities and fuel cell performance were studied. All these composition, the composition LiNiCuZn-YDC-3 shows the excellent results.

Thermo-gravimetric analysis (TGA) of composite LiNiCuZn-YDC-3 oxide material indicate that their phases are formed under 1000°C. XRD analyses are showing that the oxide materials are two phase cubic structure and their crystallite sizes increases with increasing calcination temperature. SEM and XRD results are agreed that the average crystallite size lies in the range of 10-80 nm. DC conductivities were measured in the air and hydrogen atmospheres and composite LiNiCuZn-YDC-3 oxide material shows maximum results of conductivity in hydrogen and air atmospheres. So, this material can be employed as oxygen and electron conductor. The high catalytic activity process of the LiNiCuZn-YDC-3 is a result of low activation energy. The low value of activation energy was initially produced fast chemical reaction. The electrochemical impedance spectroscopy (EIS) of the composite LiNiCuZn-YDC-3 oxide material was showed that the charge transportation, mass transportation and electro catalytic activity of the surface is improved in hydrogen atmosphere with increased the temperature range from 300 to 680 °C. Ohmic resistance (R_o), electrode polarization resistance (R_p) and total resistance (R_t) were also reduced with the increased of temperatures. High open circuit voltage and maximum power density of composite LiNiCuZn-YDC-3 oxide material was achieved by employing the hydrogen as fuel at 680 °C, to be 1.02 V and 769.54 mWcm⁻². In the end it can be concluded from these results that the composition LNCZYDC-3 oxide material can be as favorable electrode for intermediate temperature solid oxide fuel cells (IT-SOFCs).

Acknowledgements

Higher Education Commission, Pakistan (HEC) is highly acknowledged for financially support under International Research Support Initiative Program (ISRIP) to complete this work and the Department of Energy Technology, Royal Institute of Technology, KTH, Stockholm, Sweden is also acknowledged to provide all facilitations to achieve the results for the completion of work.

References

- [1] S.R. Gandavarapu, K. Sabolsky, K. Gerdes, E.M. Sabolsky, *Material Letter* **95**, 131 (2013).
- [2] S. Lee, N. Miller, K. Gerdes, *J. of The Electrochemical Society* **159**, 301 (2012).
- [3] S.P. Jiang; S.H. Chan, *Materials Science and Technology* **20**, 1109 (2004).
- [4] J.W. Kim, A.V. Virkar, K.Z. Fung, K. Mehta, S. C. Singhal, *J. of The Electrochemical Society*, **146**, 69 (1999).
- [5] W. Zhu, C. Xia, D. Ding, X. Shi, G. Meng, *Materials Research Bulletin* **41**, 2057 (2006).
- [6] X. R. Liu, B. Zhu, J. R. Xu, J. C. Sun, Z.Q. Mao, *Key Engineering Materials* **280**, 425 (2005).
- [7] B. Zhu, I. Albinsson, C. Andersson, K. Borsand, M. Nilsson, B.-E. Mellander, *Electrochemistry Communications* **8**, 495 (2006).
- [8] S. Xu, X. Niu, M. Chen, C. Wang, B. Zhu, *J. of Power Sources* **165**, 82 (2007).
- [9] J. Huang, L. Yang, R. Gao, Z. Mao, C. Wang, *Electrochemistry Communications* **8**, 785 (2006).
- [10] S. Li, X. Wang, B. Zhu, *Electrochemistry Communications* **9**, 2863 (2007).
- [11] B. Zhu, S. Li, B.-E. Mellander, *Electrochemistry Communications* **10**, 302 (2008).
- [12] B. Zhu, R. Raza, H. Qin, L. Fan, *J. of Power Sources* **196**, 6362 (2011).
- [13] B. Zhu, R. Raza, H. Qin, Q. Liu, L. Fan, *Energy & Environmental Science* **4**, 2986 (2011).
- [14] W. Shin, N. Murayam, *Materials Letters* **45**, 302 (2000).
- [15] S. Jung, K. Yong, *Chemical Communications* **47**, 2643 (2011).
- [16] Y. Xia, X. Liu, Y. Bai, H. Li, X. Deng, X. Niu, X. Wu, D. Zhou, M. Lv, Z. Wang, J. Meng, *RSC Advances* **2**, 3828 (2012).
- [17] C. M. Stoots, J. E. O'Brien, K. G. Condie, J. J. Hartvigsen, *International J. of Hydrogen Energy* **35**, 4861 (2010).
- [18] G. Marnellos, G. Karagiannakis, S. Zisekas, M. Stoukides, *Studies in Surface Science and Catalysis* **130**, 413 (2000).
- [19] Y.D. Zhen, A.I.Y. Tok, S.P. Jiang, F.Y.C. Boey, *J. of Power Sources* **178**, 69 (2008).
- [20] K.-I. Ota, S. Mitsushima, S. Kato, S. Asano, H. Yoshitake, N. Kamiy, *J. of Electrochemical Society* **139**, 667 (1992).
- [21] Y. Zhao, J. He, L. Fan, W. Ran, C. Zhang, D. Gao, C. Wang, F. Gao, *International J. of Hydrogen Energy* **38**, 16558 (2013).
- [22] J.W. Fergus, *Solid State Ionics* **177**, 1529 (2006).
- [23] J.B. Goodenough, Y.-H. Huang, *J. of Power Sources* **173**, 1 (2007).
- [24] A. Atkinson, S. Barnett, R. J. Gorte, J. T. S. Irvine, A. J. McEvoy, M. Mogensen, S. C. Singhal, *J. Vohs Nature Materials* **3**, 17 (2004).
- [25] L. Fan, C. Wang, M. Chen, B. Zhu, *J. of Power Sources* **234**, 154 (2013).
- [26] Y. Zhe, L. Qizhao, B. Zhu, *International J. of Hydrogen Energy* **35**, 2824 (2010).
- [27] L. Jia, Y. Tian, Q. Liu, C. Xia, J. Yu, Z. Wang, Y. Zhao, Y. Li, *J. of Power Sources* **195**, 5581 (2010).
- [28] M. Chen, C. Wang, X. Niu, S. Zhao, J. Tang, B. Zhu, *International J. of Hydrogen Energy* **35**, 2732 (2010).
- [29] H. Li, Q. Liu, Y. Li, *Electrochimica Acta* **55**, 1958 (2010).
- [30] B. Zhu, *J. of Power Sources* **114**, 1 (2003).
- [31] X. Wang, Y. Ma, R. Raza, M. Muhammed, B. Zhu, *Electrochemistry Communications* **10**, 1617 (2008).

- [32] H.S. Yoon, S.W. Choi, D. Lee, B.H. Kim, *J. of Power Sources* **93**, 1 (2001).
- [33] G. Abbas, R. Raza, M. Ashfaq, M.A. Chaudhry, M.A. Khan, I. Ahmad, B. Zhu, *International J. of Energy Research* **38**, 518 (2014).
- [34] S. Li, Z. Lu, B. Wei, W. Su, *Solid State Ionics* **178**, 417 (2007).
- [35] Y.M. Al-Yousef, M. Ghouse, *World J. of Nano Science and Engineering* **01**, 99 (2011).
- [36] Q.A. Huang, R. Hui, B. Wang, J. Zhang, *Electrochimica Acta* **01**, 8144 (2007).
- [37] D. Han, X. Liu, F. Zeng, J. Qian, T. Wu, Z. Zhan, *Nature* **462**, 1 (2012).
- [38] J.S. Park, I.D. Hasson, M.D. Gross, C. Chen, J.M. Vohs, R.J. Gorte, *J. of Power Sources* **196**, 7488 (2011).
- [39] T. Ishihara, H. Zhong, *Scripta Materialia* **65**, 108 (2011).
- [40] P. Blennow, K.K. Hansen, L.R. Wallenberg, M. Mogensen, *Electrochimica Acta* **52**, 1651 (2006).
- [41] S. Mutyala, M. Jayaraman, *International J. of Electrochemistry* **14**, 01 (2014).
- [42] E.J. Calvo, *Materials and Corrosion* **65**, 345 (2014).
- [43] N. Menzel, E. Ortel, R. Kraehnert, P. Strasser, *ChemPhysChem* **13**, 1385 (2012).